Mon. Not. R. Astron. Soc. **268,** 1060–1072 (1994)

The properties of cold clouds in cooling flows

S. J. Daines,[1] A. C. Fabian[1] and P. A. Thomas[2]
[1] *Institute of Astronomy, Madingley Road, Cambridge CB3 0HA*
[2] *Astronomy Centre, MAPS, University of Sussex, Falmer, Brighton BN1 9QH*

Accepted 1994 February 10. Received 1994 February 10; in original form 1991 February 5

ABSTRACT

We discuss the properties of the large masses of cold gas found in the central regions of cooling flow clusters via X-ray absorption, and explore some consequences of inefficient star formation in cooling flows. The X-ray-absorbing cold gas must be in the form of small, cold, pressure-confined clouds, which are supported against infall in the cluster potential by the hot, X-ray-emitting gas and approximately comove with it. Magnetic fields are important in supporting and containing the clouds. Cold gas deposited at large radii in the cooling flow may simply accumulate and have negligible star formation; the inner regions of the cooling flow accumulate dynamically dominant masses of cold gas on a short time-scale and some gas-removal process must be operating. We show that the constraints placed by observational detections and limits of H I and CO in some flows leave little room there for widespread cold gas in a form which is either atomic or similar to Galactic molecular clouds. Ongoing cluster mergers, or stirring produced by an intermittent central radio source, disrupt accumulated cold clouds in the core of a flow and release enough kinetic or thermal energy via cloud collisions or mixing layers to power transiently the optical emission-line nebulosity around central cluster galaxies. The large masses of disordered, clumpy, turbulent atomic gas observed near the centre of the Perseus cluster via 21-cm absorption have probably been stirred up by such an event in the past few billion years.

Key words: magnetic fields – stars: formation – galaxies: clusters: individual: Perseus – cooling flows – intergalactic medium – X-rays: galaxies.

1 INTRODUCTION

White et al. (1991) have detected large masses of cold gas in cooling flows using data from the Solid State Spectrometer on the *Einstein* satellite. The X-ray spectra show excess photoelectric absorption over that detected in our Galaxy, and require an absorbing column of $\sim 10^{21}$ cm^{-2} covering the core of the cluster out to at least ~100 kpc. This implies a cold gas mass of $\sim 3 \times 10^{11}$ M$_\odot$.

Large masses of cold gas have also recently been discovered in the inner regions of the Perseus cluster (which has a cooling flow of ~200 M$_\odot$ yr^{-1}; see Fabian et al. 1981; Allen et al. 1992) via absorption of diffuse radio emission by the 21-cm line of neutral hydrogen (Jaffe 1990, building on earlier detections by Crane, van der Hulst & Haschick 1982; Jaffe, de Bruyn & Sijbreng 1988). Using the Westerbork Synthesis Telescope, Jaffe detected a broad absorption feature of width 500 km s^{-1}, centred on the stellar velocity of 5000 km s^{-1}, at three places with a total separation of about 20 kpc centred on the nucleus of NGC 1275. He inferred a column density of $\gtrsim 1.5 \times 10^{21}\ T_{\rm c1}$ cm^{-2}, where the temperature of the H I is 10 $T_{\rm c1}$ K, which corresponds to a mass of cold gas $\lesssim 5 \times 10^{9}\ T_{\rm c1}$ M$_\odot$ within the inner ~15 kpc.

Only smaller masses of gas below X-ray-emitting temperatures have been detected in other wavebands. Up to 10^8 M$_\odot$ of ionized gas at $\sim 10^4$ K is present in some clusters within the inner few kpc, in the form of the optical line-emitting filaments (Lynds 1970; Hu, Cowie & Wang 1985; Johnstone & Fabian 1988; Heckman et al. 1989; Unger et al. 1990), although masses $< 10^6$ M$_\odot$ are more common. It is likely that the line emission is from ionized surface layers around cold clouds, which implies a greater total mass of cold gas in those regions. Molecular gas has been detected in NGC 1275 via CO emission (Lazareff et al. 1989; Mirabel & Sanders 1989), extended over about 10 kpc. The conversion factor from CO luminosity to total mass of molecular gas is uncertain. All of these detections, other than X-ray absorption, require cold gas to be present only in the centre of the cluster, at radii $R \lesssim 15$ kpc.

The consequences for the study of cooling flows (for reviews, see Fabian, Nulsen & Canizares 1984, 1991 and Sarazin 1988) of large masses of distributed cold gas are enormous. The fate of the cooling gas has long been a puzzle, as mass deposition rates integrated over a Hubble time typically give $\sim 10^{12}\ \mathrm{M}_{\odot}$. It has previously been assumed that the cooled gas forms directly into low-mass stars with high efficiency, since so little cold gas had been detected. Widespread cold clouds are a sink for the cooled gas, so that star formation need not be very efficient. The distribution of mass among the various temperature phases in a cooling flow is shown in Fig. 1.

In this paper, we first consider the properties required of widespread X-ray-absorbing material in a cooling flow. Clearly, it must be in clouds or sheets (see discussion in White et al. 1991), but the physical properties of the clouds such as temperature and density are not immediately obvious. The role of magnetic fields in supporting and binding the clouds is also of importance. We then confront data at other wavelengths, such as those obtained from 21-cm observations, to see whether the clouds have, or should have, been detected. Our overall conclusion is that there is little parameter space remaining for cold clouds that are either wholly atomic or have a warm CO content. We outline some remaining possible states for the gas.

2 THE SPATIAL DISTRIBUTION OF THE X-RAY-ABSORBING COLD CLOUDS

Here we briefly review the X-ray-absorption observations of cold gas, and compare the inferred mass and radial distribution with the mass deposited from the cooling flow.

2.1 X-ray observations of cold clouds

Cold, X-ray-absorbing gas in clusters was first discovered using data from the Solid State Spectrometer (SSS) on the *Einstein* satellite (White et al. 1991; Johnstone et al. 1992), and has since been confirmed using data from *BBXRT* (Mushotzky 1992) and *ROSAT* (Allen et al. 1993). The SSS was a non-imaging instrument with a field of view of 6

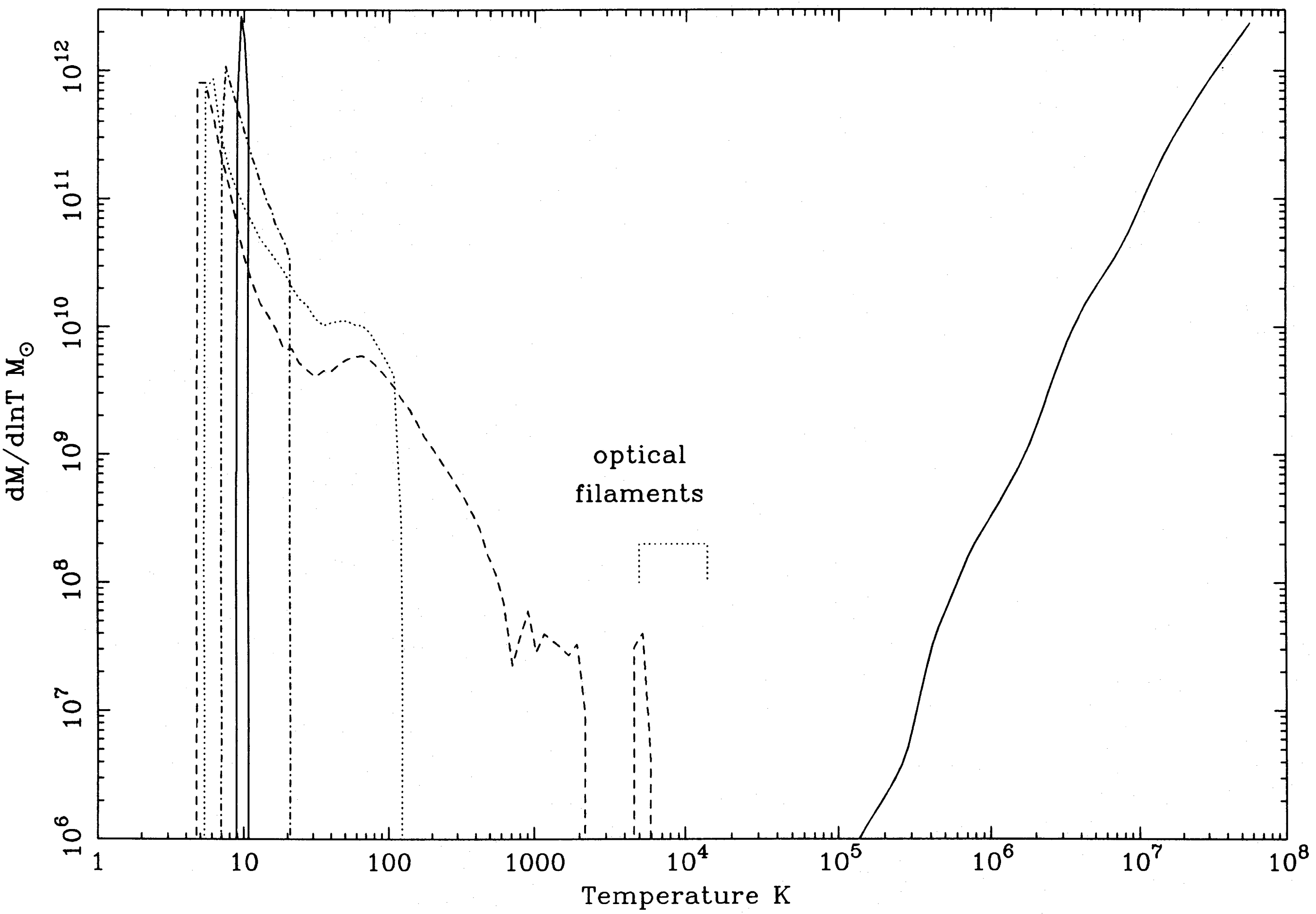

Figure 1. Distribution of mass per logarithmic temperature interval in a cooling flow. Inferred mass of hot gas with temperature in the range $10^6 < T < 10^8$ K is for a steady-state cooling flow of $\dot{M} \sim 100\ \mathrm{M}_{\odot}\ \mathrm{yr}^{-1}$ at a pressure of $4 \times 10^4\ \mathrm{cm}^{-3}$ K. Ionized gas mass with $T \sim 10^4$ K is that required to produce the observed emission-line filaments in a bright emission-line cluster such as Perseus. Four different distributions of a total mass of $3 \times 10^{11}\ \mathrm{M}_{\odot}$ of cold X-ray-absorbing gas are shown, as described in Section 3.2. These represent the thermal equilibrium of a single uniform slab column density $10^{21}\ \mathrm{cm}^{-2}$ irradiated by the cooling flow (dashed line), and three different distributions of smaller clouds with the same total line-of-sight column density and 10 (dotted), 100 (dot–dashed) and 1000 (solid line) clouds along each line of sight, respectively.

arcmin, well matched to the cooling radius of nearby clusters (3 arcmin radius corresponds to 175 kpc at a distance of 200 Mpc). All the 12 cooling-flow clusters observed required (or are consistent with) excess absorption, whereas non-cooling-flow clusters such as Coma required only the known Galactic column density. This data set demonstrates that excess absorption is a common property of cooling flows, and also requires that the cold gas is in some way associated with the cooling flow and is therefore localized within a radius of $R<300$ kpc within the cluster. The data require extra absorption corresponding to an excess column density of 10^{20}–10^{21} cm^{-2} above the Galactic value. The precise values are uncertain by about a factor of 2 due to the build-up of ice on the SSS detector. The SSS data are consistent with a partial covering model for the excess absorption, with the best data set (for A2199) requiring that the fraction of emission covered $F_c>0.6$.

Excess absorption has been confirmed in the core of the cluster A478 using spectral and spatial information from the *ROSAT* PSPC (Allen et al. 1993). The data require an excess column of $\sim 2\times10^{21}$ cm^{-2}, localized within the inner 300 kpc and implying a mass of cold gas $\gtrsim 10^{12}$ $\mathrm{M}_{\odot}$ in this object. *ROSAT* spectra of other clusters suggest that typical absorbing column densities are smaller, $\lesssim$ a few times 10^{20} cm^{-2}, on the limits of detectability with the limited spectral resolution of *ROSAT*.

The mass of absorbing gas could be reduced by a factor of a few if it directly surrounds the gas clouds cooling 1 keV and if the clouds are large. The clouds occupy about 1 per cent of the volume of the flow (taking the proportions from Fig. 1 and assuming constant pressure), and have a covering fraction less than unity only if they exceed a few kpc in radius. Such large clouds are then prone to disruption when moving relative to the hotter phase (see discussion in Section 3.3), and are therefore unlikely to exist. We conclude that the mass of cold gas cannot differ greatly from that inferred simply from the X-ray observations, assuming that the abundances of the gas are close to solar values.

2.2 Accumulation of cold gas from the cooling flow

The largest observed X-ray-absorbing column densities imply masses of 10^{11}–10^{12} $\mathrm{M}_{\odot}$, comparable to the mass deposition rate integrated over the age of the cluster, and raising the possibility that much of the cooled gas remains in the form of long-lived cold clouds. These clouds, or parts of clouds, that cause X-ray absorption are gravitationally stable (the inferred column densities are much smaller than the Jeans column density), and are not currently forming stars. They may represent either a long-lived intermediate stage, with most gas eventually forming low-mass stars on a long time-scale, or a final state for some of the gas.

The mass deposited from the cooling flow over time t, $M_c(<R)\propto Rt$, is more centrally concentrated than the hot gas, which has $M_h(<R)\propto R^2$ in the cluster core within the cooling radius (see Appendix A). The covering fraction and column density of the X-ray-absorbing screen are therefore likely to be higher nearer the centre of the flow and to decrease with increasing radius. The projected column density of accumulated cold gas within such a typical cooling flow is shown in Fig. 2 for three different cold gas accumulation (or gas removal) time-scales. Starting with a cooling flow which is initially devoid of cold clouds, the mass deposited by time t exceeds the supporting hot gas for radii $R<60(t/10^{10}\ \mathrm{yr})$ kpc (focusing of cold clouds in a constant velocity inflow leaves this result unchanged).

This last radius divides the flow roughly into two parts. In the outer part, at radii of ~ 100 kpc, the total mass of cold gas deposited by the flow is less than the mass of supporting hot gas. Cold clouds can therefore accumulate and, in order to build a column density approaching $\sim 10^{21}$ cm^{-2} from gas cooling in a typical flow (mass flow rate ≈ 1 $\mathrm{M}_{\odot}\ \mathrm{yr}^{-1}\ \mathrm{kpc}^{-1}$), must have done so for $\sim 10^{10}$ yr. Star formation from the cooling flow cannot then be more efficient than ~ 50 per cent if the age of the flow is 1–2×10^{10} yr. This requirement would be relaxed if cooling flows were stronger in the past, or if the currently observed flow also adds to the observed column by concentrating pre-existing cold clouds.

In the inner parts of a flow at radii of a few tens of kpc, dynamically dominant masses of cold gas accumulate on the shorter time-scale of a few 10^9 yr or less. It is unlikely that the hot gas can support a column density of cold gas greater than its own column density, so there must be a sink for the cold gas there (probably star formation is more efficient). The boundary of the inner region marks a transition in the behaviour of the flow within which mass loading by cold clouds becomes important. Even if the star formation time-scale $\lesssim 10^9$ yr throughout some flows, and the accumulated column density at large radius is $\lesssim 10^{20}$ cm^{-2}, too small to cause detectable X-ray absorption, it is likely that cooled material is a significant component of the intracluster medium within the inner ~ 10 kpc. We discuss some consequences of a large mass fraction of cold gas in the inner regions of the flow later (see Section 3.4). Note that the inner region is only a small fraction of the whole flow and is not yet well resolved by X-ray spectroscopic observations. Thus, although the loading of the flow by cold clouds should increase the temperature of the hot phase there, the overall effect is small and consistent with observations.

3 THE PHYSICAL STATE OF THE X-RAY-ABSORBING MATTER

We now explore models for the X-ray-absorbing matter. Although gas cooling from X-ray temperatures absorbs photons in the energy range around 0.5 keV as soon as the temperature drops below $\sim 5\times10^6$ K, and most oxygen atoms retain one or more electrons, the cooling rate at such temperatures is so fast that there is not enough gas to produce detectable absorption. Significant absorption can only come from a reservoir of gas at lower temperatures in thermal equilibrium. (The mass of gas above $\approx 10^6$ K determined by the constant-pressure cooling rate is shown in Fig. 1). The behaviour of the cooled gas at lower temperatures depends on whether or not thermal gas pressure dominates magnetic pressure. The weak intracluster magnetic field (supplying $\lesssim 10^{-2}$ of the thermal pressure in the hot phase) is amplified as the gas cloud cools, and can then reach pressure equilibrium at temperatures of 10^4–10^6 K (see, e.g., Richer et al. 1993). If the magnetic field configuration is stable, the gas in such clouds will continue to cool at approximately constant density until reaching thermal equilibrium with the energy input from the hot X-ray phase. Whether significant masses of gas can remain in this low-density state

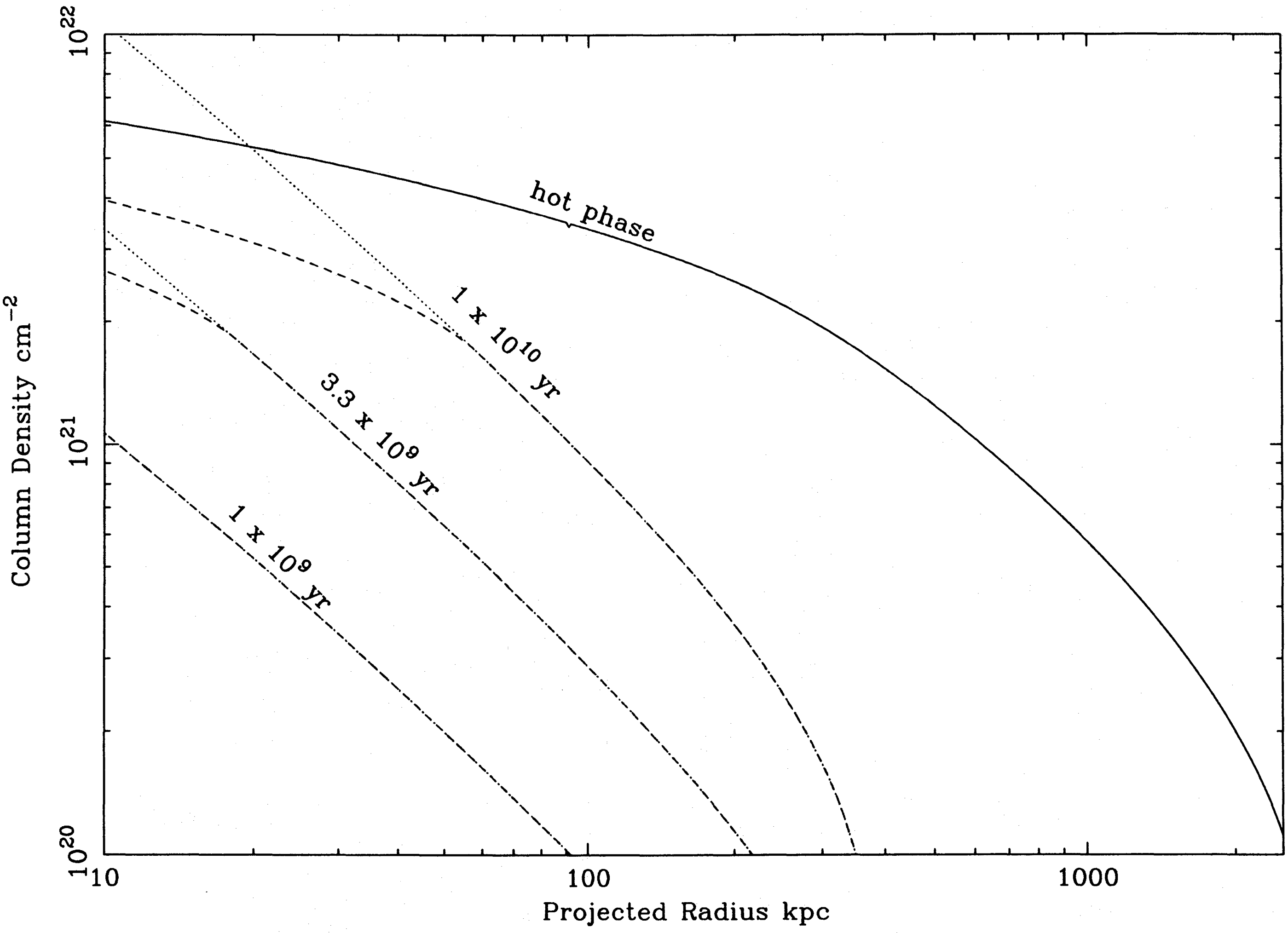

Figure 2. Column density of hot and cold phases of the ICM (line-of-sight column divided by 2). The column density of hot gas (solid line) is from Appendix A. Dotted lines represent the column density of cold gas accumulated from a cooling flow of 1 $M_\odot$ yr^{-1} kpc^{-1}, assumed to continue out to 400 kpc after three different times, if all the cold gas remains where it cools out of the flow. Dashed lines represent the cold gas accumulated if the averaged density of the cold gas is limited to be less than the mean density of hot gas.

is not clear. If gas pressure continues to dominate as the gas cools, the gas temperature rapidly drops to very much lower values (Ferland, Fabian & Johnstone 1994) as the gas density rises to remain in pressure equilibrium. A final possibility for the X-ray-absorbing matter is that cloud cores lose their magnetic field and become so dense and cold that dust grains form. Much of the gas then freezes on to these grains, so that the matter is part solid, part gas. This possibility is pursued elsewhere (Fabian, Daines & Johnstone 1994).

In Section 3.1, we discuss the properties of low-density, magnetically dominated clouds (which must at least represent an intermediate stage for the cooling gas), and, in Section 3.2, we discuss the implications of the results of Ferland et al. (1994) for small, cold, dust-free clouds dominated by thermal pressure, which have column densities similar to those inferred from X-ray absorption. In Section 3.3, we discuss the physical state of cold clouds and their interaction with the hot phase at large radius in the cooling flow. In Section 3.4, we explore some consequences of cloud–cloud interactions in the inner regions of the flow, where the mass fraction of cold gas is higher and cloud collisions become important, and discuss the relationship between material cooled from the cooling flow and the emission-line nebulosity observed near the centres of many clusters.

3.1 The temperature of magnetically dominated clouds

The magnetic pressure in the hot phase of the intracluster medium is typically about 1 per cent of the total pressure throughout the bulk of the intracluster medium (with typical fields of μG; Kim, Tribble & Kronberg 1991), and may be stronger in the inner ~10 kpc (e.g. Ge & Owen 1993). The magnetic pressure rises as the gas cools, at a rate which depends on the geometry of the field, but it can easily dominate the total pressure of the cooling blob at temperatures of 10^4–10^6 K. Below the temperature where it dominates, the gas cools at constant density (say about 0.1 cm^{-3}) to a temperature determined by the heating rate of the incident X-rays. Using Ferland's (1993) code CLOUDY, we find that the resultant cloud would have a completely ionized skin of thickness 6×10^{18} cm^{-2} and temperature 10^4 K, and an

1994MNRAS.268.1060D

inner region of up to 6×10^{20} cm^{-2} which is at $\sim 10^3$ K. Thus substantial clouds could exist which have most of their gas at temperatures approximately greater than 10^3 K.

3.2 Clouds dominated by thermal pressure

We show, in Fig. 1, the distribution of cold gas mass as a function of temperature for four different assumptions about the spatial distribution of the X-ray-absorbing material through the hot X-ray-emitting phase. In each case the cold gas (assumed dust-free) is at its equilibrium temperature, maintained by heating from absorbed X-rays. We first reproduce the results of Ferland et al. (1994) using the same computer code (CLOUDY), for a uniform cold slab of column density 10^{21} cm^{-2} (we scale the masses to correspond to a total of 3.3×10^{11} M$_\odot$, which is the mass of a circular slab of radius 100 kpc). The incident continuum is calculated as the radiation from a sum of collisional-equilibrium thermal plasma spectra representing the cooling at constant pressure of 100 M$_\odot$ yr^{-1} spread over the area of a sphere with radius 100 kpc (we assume abundances at 0.4 solar and a pressure 4×10^5 cm^{-3} K – see Appendix). The front face of the slab has a small mass of gas $\approx 2 \times 10^7$ M$_\odot$ at temperature $\approx 5 \times 10^3$ K, partially ionized with ionization fraction ~ 0.1; it then becomes progressively colder with increasing depth as the incident continuum is attenuated and the heating rate declines. The temperature drops to 4.1 K at a depth of 10^{21} cm^{-2}, and some of the hydrogen forms molecules with the molecular fraction reaching 22 per cent by mass. 99 per cent of the total mass is colder than 84 K and 90 per cent is below 8.9 K.

The X-ray-absorbing material is more likely in practice to be distributed in many small clouds throughout the emitting volume, with a large number of clouds along each line of sight. The face of each cloud 'sees' the total emitted flux absorbed by other clouds along the line of sight, and the heating rate is then more evenly distributed through the volume of the cloud as shielding by the ensemble of clouds becomes more important than self-shielding with increasing depth inside an individual cloud (the incident spectrum becomes harder due to absorption by clouds along the line of sight). We illustrate this effect by calculating the thermal structure of clouds modelled as a plane-parallel sandwich of f_c clouds, individually of column density $10^{21}/f_c$ cm^{-2}, and each irradiated by the total emitted continuum attenuated by the factor

$$a_\nu = \frac{1}{f_c+1}\,\frac{1-\exp[-(f_c+1)\,\tau_\nu]}{1-\exp(-\tau_\nu)}, \qquad (1)$$

where τ_ν is the optical depth of an individual cloud at frequency ν. We show the temperature distribution for $f_c = 10$, 100 and 1000 clouds. As the number of clouds along each line of sight increases, the temperature of an individual cloud becomes more uniform, and converges to a limit determined by the balance between the overall X-ray heating rate and cooling (which is via the optically thin C I 610-μm line in this model). The cloud with column density 10^{18} cm^{-2} has temperature ≈ 10 K, ionization fraction $x_1 \approx 2 \times 10^{-5}$, and hydrogen molecular fraction 0.15 by mass.

The distribution of gas mass as a function of temperature must lie between the two extremes of a single absorbing slab and a uniform distribution of small clouds, and we may draw some general conclusions from the above results. Most of the mass will be cold, with over 90 per cent below 10 K. The Jeans mass is then $0.3 P_6^{-2} T_{c1}^2$ M$_\odot$, where the temperature of the cold phase is $10 T_{c1}$ K, and the cloud radius as a function of column density $10^{21} N_{c21}$ cm^{-2} is $r_c = 0.0015 N_{c21} P_6^{-1} T_{c1}$ pc. Dust-free clouds do form some molecular hydrogen, but the X-ray radiation field in a cooling flow is sufficient to keep more than 80 per cent of the hydrogen atomic.

3.3 Interactions between cold clouds and the hot phase

Cold clouds are greatly overdense with respect to the ambient medium, and must be supported against infall in the cluster potential by being suspended in the hot gas. They cannot orbit ballistically, as they would be rapidly slowed down either by ram-pressure drag from the hot gas (stopping length in the hot gas $30 N_{c21} n_{h-2}$ kpc) or by collisions with other clouds (as the number of clouds along each line of sight must exceed unity). We note that, even for the case of thermal-pressure-dominated clouds, there are no solutions for long-lived clouds that do not involve magnetic fields. Any unmagnetized cloud (unless very close to its Jeans mass) is rapidly disrupted by Rayleigh–Taylor forces (Nulsen 1986; Mathews & Murray 1987; Loewenstein & Fabian 1990) and evaporated by conduction at the Spitzer rate. The details of the interaction between cold clouds and the hot phase then depend on the magnetic field geometry. We envisage two field configurations as models for the dynamical state of the clouds: (i) the cloud is penetrated and supported by the intracluster magnetic field, with clouds hanging in loops in the field lines, and (ii) clouds are held together by closed internal field lines, and exist in the form of small ram-pressure-supported droplets falling on average at their terminal velocity (like rain). In either case, the cold gas is tied to the field lines by ambipolar diffusion relative to the residual ionized fraction maintained by X-ray irradiation from the surrounding gas.

The intracluster magnetic field is observed to have a magnitude of a few μG from observations of Faraday rotation of background radio sources (Kim et al. 1991) and therefore contributes a pressure or tension $P_{\rm mag}$ which is a fraction $\sim 10^{-2}$ of the thermal pressure $P_{\rm therm}$. Taking this estimate of the field strength (which is a lower limit, since the field lines may well be concentrated inside or nearby clouds), we may estimate the range of plausible cloud sizes. In model (i), the magnetic tension from field lines leaving the cloud must support it against gravity. As the thermal pressure of the hot gas supports a column $N_h \sim 10^{21}$ cm^{-2} per scaleheight in the cluster potential, magnetic tension is able to support the weight of a cold cloud with column density $N_c < (P_{\rm mag}/P_{\rm therm}) N_h \lesssim 10^{19}$ cm^{-2}. There is either a large number of such clouds along each line of sight, or $P_{\rm mag} \sim P_{\rm therm}$, in order to provide observable X-ray absorption.

In model (ii), the internal cloud field could either permeate the whole cloud or be confined to a thin ionized skin. In either case, it must provide sufficient tension to hold the cloud together against the excess internal pressure $\sim N_c/N_h P_{\rm therm}$ caused by the weight of the cloud. If a field of a few μG permeates the whole cloud, then the maximum cloud size is $N_c < (P_{\rm mag}/P_{\rm therm}) N_h$, as derived in the previous paragraph. If the field is confined to an ionized skin with column density N_i around a thermal-pressure-dominated cloud, then a given field can hold together a smaller cloud with column density reduced by the fraction of cloud cross-sectional area that is ionized. With the density of the cold core at 10 K being 1000 times the density of the ionized skin at $\sim 10^4$ K, the cloud column density is $N_c \lesssim 10^3 (N_i/N_c)(P_{mag}/P_{therm}) N_h$. If the skin retains a field strength comparable to the thermal equipartition value, then an ionized skin $N_i \sim 10^{16}$ cm^{-2} can contain a cloud with $N_c \lesssim 10^{20}$ cm^{-2}. Such clouds will fall on average at the terminal velocity (where ram pressure balances the weight of the cloud) such that $v^2_{term}/v^2_s \sim N_c/N_h$, where the sound speed in the hot phase is v_s. A mist of small clouds, $N_c \lesssim 10^{19}$ cm^{-2}, with terminal velocities $\lesssim 100$ km s^{-1} could then remain at large radius for $\gtrsim 10^9$ yr (the time to fall 100 kpc) and accumulate sufficient mass to cause observable X-ray absorption. Larger clouds could contribute if the clouds were redistributed out to large radii, as the cluster core is periodically stirred up and disrupted by subcluster mergers.

3.4 Consequences of cloud–cloud interactions in the inner regions

As discussed in Section 2.2, the core of a cooling flow (i.e. the innermost few kpc) soon accumulates a mass of cooled gas comparable to the mass of hot gas. In this situation the cold clouds must dominate the dynamics.

A first consequence of the accumulation of dynamically significant masses of cold clouds is that coagulation (and subsequent star formation as clouds are pushed over the Jeans mass) will become more efficient as a result of a combination of dissipative cloud collisions and some re-acceleration. Cloud collisions will always be dissipative (as shocked gas rapidly cools). However, coagulation will only occur if collision velocities are low, relative to the internal sound speed of the clouds, as collisions will always be slightly messy with some residual kinetic energy and momentum (Gilden 1984). This may be achieved by the interaction between the hot and cold phases in the following manner, analogous to thermal instability. We assume that cold clouds are moving around, and supported, in a global sense, by a hot phase, and that the two phases have similar (averaged) mass densities. If the number density of cold clouds is ψ_c, the kinetic energy injection rate per unit volume from the hot phase into the cold phase is proportional to ψ_c, and the dissipation rate of kinetic energy in the cold phase via collisions is proportional to ψ_c^2. A region containing an excess of cold clouds therefore loses kinetic energy, and all phases move slower than average. Clouds therefore enter the region faster than they leave, perpetuating the excess. Clouds in such a region then have low relative velocities and can coagulate into larger clouds. Such a combination of acceleration by 'noise' in the intracluster medium (ICM) and dissipative cloud collisions should also produce large-scale clumps and structures in the cold-cloud population.

Secondly, the presence of large accumulated masses of cold gas facilitates mechanisms for powering the optical emission-line nebulosity observed near the centres of some clusters. Approximately 40 per cent of cooling-flow clusters show optical activity, with the bolometric luminosity L_{neb} of the optical nebulae relative to the X-ray luminosity of the cooling flow L_{cool} typically ranging from $L_{neb} = 0.01$–$0.1\,L_{cool}$ (Heckman et al. 1989) up to rare examples such as Perseus showing $L_{neb} \sim L_{cool}$ (note that the optical line luminosity is localized within the inner few tens of kpc of the flow and then far exceeds the X-ray luminosity from the same region in clusters such as Perseus). Large masses of cold gas facilitate the production of emission-line nebulosity either via cloud collisions (utilizing kinetic energy of the ICM) or via mixing layers on cloud surfaces (draining more thermal energy from the hot gas), and a combination of these two provides a fit to observed spectra (Crawford & Fabian 1992). Low levels of emission-line nebulosity could be powered continuously by dissipating the kinetic energy of focused sound waves (Pringle 1989; the increasing mean density towards the cluster centre, due to the centrally concentrated cold clouds, assists with this mechanism), or could drain thermal energy from the hot gas without affecting the structure of the cooling flow (mixing will also be enhanced by 'noise' in the ICM).

Stirring and increased turbulence will follow a subcluster merger or the switching on of a central radio source and cause cloud collisions, coagulation and star formation from the previously accumulated population of cold clouds. The cold-gas content of cooling flows may thereby be time-variable, with mergers periodically sweeping the flow clear of accumulated cold clouds. The brightest emission lines in Perseus and similar clusters are likely to be transient and represent the dissipation of stored thermal energy, and/or the kinetic energy of the ICM, on a dynamical time-scale during a merger. The maximum power available from mass M_h of hot gas at temperature T_h released on a crossing time l/v by mixing with disrupted cold clouds is then

$$L_{max} \sim 5 \times 10^{44} \left(\frac{M_h}{5 \times 10^{10}\,M_\odot}\right)\left(\frac{l}{20\,\mathrm{kpc}}\right)\left(\frac{v}{300\,\mathrm{km\,s^{-1}}}\right)^{-1} \times \left(\frac{T_h}{5 \times 10^7\,\mathrm{K}}\right)\mathrm{erg\,s^{-1}}, \qquad (2)$$

comparable to the total (inferred) line luminosity of the nebulosity at the centre of the Perseus cluster. A similar reservoir of energy is available in the form of kinetic energy if the ICM is stirred up to transonic velocities, and this could similarly be released on a dynamical time-scale via collisions between large masses of accumulated cold clouds.

4 CONSTRAINTS ON COLD CLOUDS FROM OBSERVATIONS IN NON-X-RAY BANDS

In this section, we confront the expected observational signature of the clouds described in Section 3 with available observational constraints in the 21-cm line of H I and the millimetre-wave CO band. 21-cm emission and absorption and CO emission have so far been detected only in the inner few tens of kpc of cooling-flow clusters, where the cold gas clouds are likely to have very different properties from the more widespread gas in the X-ray absorbing screen. Stringent upper limits exist on widespread cold atomic gas in a few clusters.

We begin by giving a formal discussion of the 21-cm signature of cold clouds, emphasizing the likely differences from detected clouds in our Galaxy. We then discuss the available data in H I and CO bands.

1994MNRAS.268.1060D

4.1 21-cm constraints on neutral hydrogen

4.1.1 The 21-cm signature of cold clouds

The interpretation of 21-cm observations of cooling flows is complicated by the fact that an individual cloud is far too small to be spatially resolved, and the whole population of clouds may have such a broad total linewidth that it is not spectrally resolved as a line. Clouds may also be highly optically thick.

Individual clouds of radius $r_c \sim 0.0015(N_c/10^{21}\ \mathrm{cm}^{-2})\ P_6 T_{c1}^{-1}$ pc subtend an angle of a few microarcsec at a nearby cluster distance of 100 Mpc. This is much smaller than any attainable telescope resolution, and smaller also than the possible size of any background radio source at 21 cm (a radio source with 21-cm flux F and brightness temperature T_b has an angular size corresponding to a linear dimension of $0.4(D/100\ \mathrm{Mpc})(F/1\ \mathrm{Jy})^{1/2}(T_b/10^{12}\ \mathrm{K})^{-1/2}$ pc, where D is the cluster distance, and the Compton catastrophe limits the brightness temperature to $T_b < 10^{12}$ K). Absorption and emission measurements will average over many clouds and produce broad spectral features determined by the overall velocity width of the cloud population ΔV rather than the narrow thermal width of an individual cloud. The emission (or absorption) profile produced will be smooth providing the telescope beam (and overlap with background radio source) contains many more clouds than there are correlator channels within the linewidth.

Linewidths may well be large, as the cold clouds comove with the hot phase, which may be turbulent or contain large-amplitude sound waves. The FWHM of the resulting line profile (assumed Gaussian) will be $\Delta V_{\mathrm{FWHM}} = 1175 M(\sigma/500\ \mathrm{km\ s^{-1}})\ \mathrm{km\ s^{-1}}$, where M is the ratio of bulk velocities in the ICM to the hot-phase sound speed, or equivalently the galaxy velocities. The dynamical state of the ICM is unknown, although there is evidence from the linewidths of optical line nebulosity in the inner few tens of kpc in some flows that at least the inner regions are turbulent. One indication that linewidths may be large comes from the observed linewidth of H I emission in the E0 galaxy M86 (Bregman & Roberts 1990), showing that in this object $M = 0.4$. If the bulk motions in the ICM were of comparable Mach number to those in the interstellar medium of M86, linewidths could be very large, i.e. $\Delta V_{\mathrm{FWHM}} \gtrsim 600\ \mathrm{km\ s^{-1}}$.

A further complication is that individual clouds may be optically thick. The optical depth of an individual cold atomic cloud is given in terms of the column density of atomic gas N_{H} by

$$\int \tau\, \mathrm{d}v = \left(\frac{N_{\mathrm{H}}}{1.83\times 10^{19}\ \mathrm{cm}^{-2}}\right)\left(\frac{T_s}{10\ \mathrm{K}}\right)^{-1}\ \mathrm{km\ s^{-1}}, \qquad (3)$$

(see, e.g., Kaplan & Pikelner 1970), where the spin temperature T_s specifies the relative level populations, and will be equal to the kinetic temperature at the high density of cold gas in a cooling flow (Field 1958). The linewidth of an individual cloud will be dominated by the thermal width, giving a Gaussian profile with full width at 1/e of maximum depth $\Delta v_c = 0.82\, T_{c1}^{0.5}\ \mathrm{km\ s^{-1}}$. Defining the mean optical depth by $\tau_c = \int \tau\, \mathrm{d}v/\Delta v_c$, we then have $\tau_c = (N_{\mathrm{H}}/1.50\times 10^{19}\ \mathrm{cm}^{-2})\, T_{c1}^{-3/2}$. As pointed out by Loewenstein & Fabian (1990), at the high pressure of a cooling flow, Jeans-stable clouds can be highly optically thick, with the Jeans column corresponding to an optical depth $\approx 600 P_6 T_{c1}^{-3/2}$.

If the individual clouds are optically thin, $\tau_c \ll 1$, then the 21-cm signature of the atomic gas in the cloud population is directly related to the total mass and assumed temperature, and we have the standard results that the absorption optical depth is $\tau_{\mathrm{obs}} = (N_{\mathrm{av}}/2\times 10^{18}\, T_s\ \mathrm{cm}^{-2})/\Delta V$, and the emission brightness temperature above the microwave background at T_{MWB} is $\Delta T_b = (N_{\mathrm{av}}/2\times 10^{18}\ \mathrm{cm}^{-2})(1 - T_{\mathrm{MWB}}/T_s)/\Delta V$ K.

If the clouds are optically thick, $\tau_c > 1$, then the observational signature per unit mass is reduced, approximately, by the factor τ_c, allowing larger masses of atomic gas to be hidden from observation. The observed signature of an optically thick population is now directly related to the number of clouds along each line of sight f_c and temperature, rather than the gas mass, giving

$$\tau_{\mathrm{obs}} = f_c(\gamma \Delta v_c/\Delta V)(1 - \mathrm{e}^{-\tau_c}), \qquad \tau_{\mathrm{obs}} \ll 1, \quad (4)$$

$$\Delta T_b = f_c(\gamma \Delta v_c/\Delta V)(T_s - T_{\mathrm{MWB}})(1 - \mathrm{e}^{-\tau_c})\ \mathrm{K}, \qquad \tau_{\mathrm{obs}} \ll 1. \quad (5)$$

The optically thick screen we have described behaves both for emission and absorption as a homogeneous, optically thin slab with $\tau = \tau_{\mathrm{obs}}$, as given by equation (5). We have assumed $f_c \Delta v_c/\Delta V < 1$, so we expect $f_c \gg 1$, but have assumed that, although clouds may overlap along the line of sight, they do not also overlap in velocity. We have also assumed that the curve-of-growth is completely flat once the line profile saturates [the correction factor γ varies from unity for $\tau_c \ll 1$ to $\log^{1/2}(2\tau_c/\pi^{1/2})$ in the limit of high optical depth, with $\gamma \approx 2.5$ at $\tau_c = 100$].

4.1.2 Constraints on cold atomic gas in the X-ray-absorbing material

21-cm upper limits towards cooling flows have been obtained by Burns, White & Haynes (1981), Valentijn & Giovanelli (1982), Jaffe et al. (1988), Bregman, McNamara & O'Connell (1990) and Jaffe (1990, 1991, 1992). In addition, there exist some upper limits from earlier observations towards clusters which later turned out to be cooling flows, by Penzias & Scott (1968), Allen (1969a,b), Haynes, Brown & Roberts (1978) and Baan, Haschick & Burke (1978) – we note a probable typographical error in the last paper and take the upper limits obtained as a factor of 10 above those quoted. The majority of the observations above had sensitivity only to relatively narrow linewidths $\Delta V \lesssim 400\ \mathrm{km\ s^{-1}}$, and are stringent enough to rule out masses and covering fractions of atomic gas sufficient to cause the observed X-ray absorption with such linewidths. However, it is likely that linewidths in the ICM exceed those to which many of these observations were sensitive, if the ICM is either turbulent or contains large-wavelength sound-waves or bulk motions across the ~100-kpc scale of the X-ray-absorbing material. The most interesting constraints on the properties of widespread X-ray-absorbing material therefore come from the few 21-cm observations sensitive to broader linewidths.

We show the three strongest limits, in A2052 (Jaffe 1991), A2063 (Valentijn & Giovanelli 1982) and M87 (Allen 1969a,b), in Table 1 and Fig. 3. In each case, the limits are scaled to an assumed FWHM, $\Delta V = 900\ \mathrm{km\ s^{-1}}$. For A2052 and A2063, this is near the maximum linewidth to which

Table 1. 21-cm upper limits on atomic gas.

	$\dot{M}$	σ	sensitivity ΔV FWHM	$N_{\rm thin}$ ($\tau_{\rm c} \ll 1$)	$f_{\rm c}$ ($\tau_{\rm c} \gg 1$)	$\times \Delta V$
	$\mathrm{M_{\odot}\,yr^{-1}}$	$\mathrm{km\,s^{-1}}$	$\mathrm{km\,s^{-1}}$	$\times 10^{19}\,\mathrm{cm^{-2}}$		
A2052	402[1]	576 [2]	< 400[5]	$< 0.43 T_{\rm c1}$	$< 0.5(T_{\rm c}/T_{\rm MWB})^{-1/2}$	$\times(\Delta V/400\,\mathrm{km\,s^{-1}})$
M87	10[1]	760 [4]	> 60[7]	$< 2.7 T_{\rm c1}$	$< 6(T_{\rm c}/T_{\rm MWB})^{-1/2}$	$\times(\Delta V/900\,\mathrm{km\,s^{-1}})$
A2063	45[1]	652 [3]	< 900[6]	$< 6(1 - T_{\rm MWB}/T_{\rm c})^{-1}$	$< 23(T_{\rm c}/T_{\rm MWB})^{-3/2}$ $(1 - T_{\rm MWB}/T_{\rm c})^{-1}$	$\times(\Delta V/900\,\mathrm{km\,s^{-1}})$

Limits are from absorption for A2052 and M87, and from emission for A2063 (see text). Column 4 gives the claimed linewidths to which the observations were sensitive. Columns 5 and 6 interpret these limits as upper limits to the column density $N_{\rm thin}$ of optically thin H I, and the covering fraction of optically thick H I clouds $f_{\rm c}$, respectively. These should be scaled by the assumed linewidth as in column 7. The cold gas has temperature $T_{\rm c}$ which must exceed the microwave background temperature $T_{\rm MWB}$.

[1] Edge, Stewart & Fabian (1992), [2] Quintana et al. (1985), [3] Zabludoff, Huchra & Geller (1990), [4] Binggeli, Tammann & Sandage (1987), [5] Jaffe (1991), [6] Valentijn & Giovanelli (1982), [7] Allen (1969b).

these observations were sensitive. The observation towards M87 was originally carried out to search for neutral hydrogen anywhere between us and Virgo, and is sensitive to arbitrarily broad linewidths.

The absorption observation of A2052 was carried out with a beam size of 14×100 kpc^2 in front of a diffuse background radio source extended on a scale of 100 kpc. The Arecibo emission limit towards A2063 was obtained with a beamsize corresponding to a radius of 97 kpc at the assumed distance of A2063. Both these observations must have therefore obtained a fair sample of a putative X-ray-absorbing screen. Unfortunately, neither cluster was included in the SSS sample, and there is no direct evidence for X-ray absorption, although with $\dot{M} \approx 90$ and ≈ 45 $\mathrm{M_{\odot}\,yr^{-1}}$ we may expect these objects to represent typical medium-sized cooling flows. M87 is a very much smaller cooling flow, $\dot{M} \approx 10$ $\mathrm{M_{\odot}\,yr^{-1}}$, although it does have a measured SSS column density of $\approx 1.5 \times 10^{21}$ cm^{-2}. The interpretation of the 21-cm observation of M87 is somewhat ambiguous, as the structure of the background radio source is complicated. The background radio source consists of a compact central region $R < 3$ kpc supplying ≈ 60 per cent of the total flux at 21 cm, and a halo radius ≈ 30 kpc supplying the rest. The SSS beam covers a radius of 18 kpc for an assumed Virgo distance of 20 Mpc, and a clumped distribution of X-ray-absorbing material in this beam need only cover $\sim 1/5$ of the radio emission.

If we assume that the clouds are cold, $T \lesssim 1000$ K, we see from Fig. 3 that the A2052 limit is sufficiently tight to rule out marginally even a screen of optically thick atomic clouds with the minimum covering fraction $f_{\rm c} \gtrsim 1$ required to cause observable X-ray absorption. The other limits are somewhat less restrictive, but still allow little parameter space for any cold population of primarily atomic clouds capable of causing observable X-ray absorption. The 21-cm absorption signature is greatly reduced if the cloud temperature was higher, $T \sim 10^3$ K, as expected if the clouds were of lower density and dominated by magnetic pressure (the spin temperature could then also be pushed to temperatures higher than the kinetic temperature by a bright central radio source). However, this has no effect on the 21-cm emission per unit mass, and the A2063 limit remains equally restrictive for warm gas.

4.1.3 21-cm detections in cooling flows

The status of 21-cm observations of cooling flows is further confused by the fact that patches of atomic gas have been detected in four clusters, although all are consistent with absorption or emission by atomic gas within the inner 15 kpc and the relationship of these detections to the X-ray absorbing screen is obscure.

The two 21-cm detections where the absorption and emission are spatially mapped (in NGC 1275 and M87; Jaffe 1990, 1992) are of atomic gas nearer the centre of the cooling flow than required to produce the X-ray absorption, and spatially associated with the optical line-emitting nebulosity. The two 21-cm detections in MKW3s and 2A0335+096 (summarized in Table 2) were made with the broad Arecibo single beam in front of spatially extended radio sources, and the spatial distribution of the absorbing gas is therefore unknown. Most of the flux from the background radio source in MKW3s comes from an extended, steep-spectrum source, offset from the central cD by ≈ 50 arcsec (64 kpc). However, the radio structure within the telescope beam also indicates a small point source centred on the cD, supplying 6 mJy out of the total flux of 110 mJy (unpublished VLA data, Fomalont & Miley, private communication), and further observations have shown the absorption to be due to H I covering the nucleus only (Jaffe 1993).

The properties of cold clouds may be very different in the inner regions of the cooling flow, where the presence of emission-line filaments shows that further heating sources are present in addition to X-ray irradiation from the surrounding hot gas. It is nevertheless puzzling that apparently stringent upper limits to the H I content exist in other bright emission-line clusters which have been observed at 21 cm (such as A1795, where the line emission covers most of the radio source and an apparently tight 21-cm

Table 2. 21-cm detections in cooling flows.

	$\dot{M}$ $M_\odot$ yr^{-1}	τ_{obs}	ΔV km s^{-1}	line centre km s^{-1}	N_{thin} ($\tau_c \ll 1$) $\times 10^{19}$ cm^{-2}	f_c ($\tau_c \gg 1$)
MKW3s	151 [1]	0.02 [2]	117	-90	$2.4T_{c1}$	$2.9T_{c1}^{-1/2}$
2A0335+096	142 [1]	0.014 [2]	270	-237	$2.2T_{c1}$	$2.9T_{c1}^{-1/2}$
NGC 1275 (off-nucleus)	183 [1]	0.15 [3]	500	0	$150T_{c1}$	$98T_{c1}^{-1/2}$
NGC 1275 (on-nucleus)	183 [1]	0.0021 [3]	500	0	$2.1T_{c1}$	$1.4T_{c1}^{-1/2}$

Data are from observations with the Arecibo single dish by McNamara et al. (1990) [2] and WSRT interferometer by Jaffe (1990) [3] (see text). Mass deposition rates [1] are from Edge et al. (1992). Column 6 gives the column density N_{thin} of H I at temperature 10 T_{c1} K required to produce the observed absorption feature of optical depth τ_{obs} over linewidth ΔV, if this is assumed to be optically thin. Column 7 gives a minimum covering fraction f_c of clouds if assumed optically thick.

absorption limit exists, from McNamara, Bregman & O'Connell 1990). We suggest that these observations may have missed large quantities of cold atomic gas near the cluster centre due to an insensitivity to broad linewidths.

4.2 Millimetre constraints on CO

Upper limits on CO emission (and sometimes absorption) in the $J=1-0$ and $J=2-1$ millimetre transitions have been obtained towards cooling flow clusters by Jaffe (1987), Bregman & Hogg (1988), Grabelsky & Ulmer (1990), McNamara & Jaffe (1994) and O'Dea et al. (1994). CO emission has definitely been detected only in the inner ≈ 15 kpc of NGC 1275 (Lazareff et al. 1989; Mirabel et al. 1989). The observational situation with CO millimetre emission and absorption is therefore similar to that for the H I 21-cm line, namely one or a few detections near the centre of the cooling flow region and of similar spatial scale to the emission line nebulosity, and upper limits on the CO signature of cold gas as widespread as required to cause observable X-ray absorption.

The tightest CO emission upper limits require antenna temperatures $\lesssim 5-10$ mK, with the same caveats about possible broad linewidths as discussed above for the H I 21-cm line (O'Dea et al. 1994; McNamara & Jaffe 1994; the latter authors discuss their sensitivity to broad linewidths ≈ 900 km s^{-1}). These upper limits imply masses of $\lesssim 10^8-10^9$ $M_\odot$ of molecular gas with a Galactic CO to mass conversion factor. However, the CO signature of cold gas in a cooling flow will be very different from that of molecular clouds in our Galaxy. We may make the same argument about the minimum observational signature of a screen of optically thick clouds as for the H I 21-cm line. The available upper limits of $\lesssim 5-10$ mK then imply gas temperatures of $\lesssim 10$ K for a required number of clouds along each line of sight exceeding unity (see Fig. 3).

In the context of the pressure-confined cloud model, these limits are not restrictive. As discussed in Section 3.2, we find that dust-free clouds have temperatures $\lesssim 10$ K, and form negligible CO (the gas remains primarily atomic). Preliminary results for clouds containing dust indicate that the gas then becomes highly molecular but very cold indeed with temperature ~ 3 K, very close to the microwave background temperature and therefore undetectable in emission (Fabian et al. 1994).

5 NGC 1275 AS AN EXAMPLE OF CLOUD PROPERTIES IN THE INNER REGIONS

Large masses of atomic gas have been observed in 21-cm absorption in the inner 15 kpc of the cooling flow around NGC 1275 by Jaffe (1990). This observation complements the existing X-ray-absorption observations of widespread cold gas by providing evidence for large masses of cold gas nearer the cluster core. NGC 1275, the central galaxy in the Perseus cluster, is surrounded by a bright optical emission-line nebula and also has a population of young blue star clusters interpreted as recently formed globular clusters (Holtzmann et al. 1992; Richer et al. 1993). In a cooling-flow model, the optical emission and visible star formation are due to the mixing, collisions and coagulation of accumulated cold gas. The 21-cm observations support this picture by providing evidence for large masses of accumulated cold gas, and demonstrate that the dynamical state of the clouds is complicated, with a short collision mean-free-path and (as we demonstrate here) a clumped distribution. We suggest that the observed complicated dynamical state of the clouds around NGC 1275 is transient and due to stirring by the central radio source or a recent cluster merger. NGC 1275 is therefore not a typical example of a cooling flow; it is just the nearest large one which is well studied and for which recent activity makes much of the cold gas content visible.

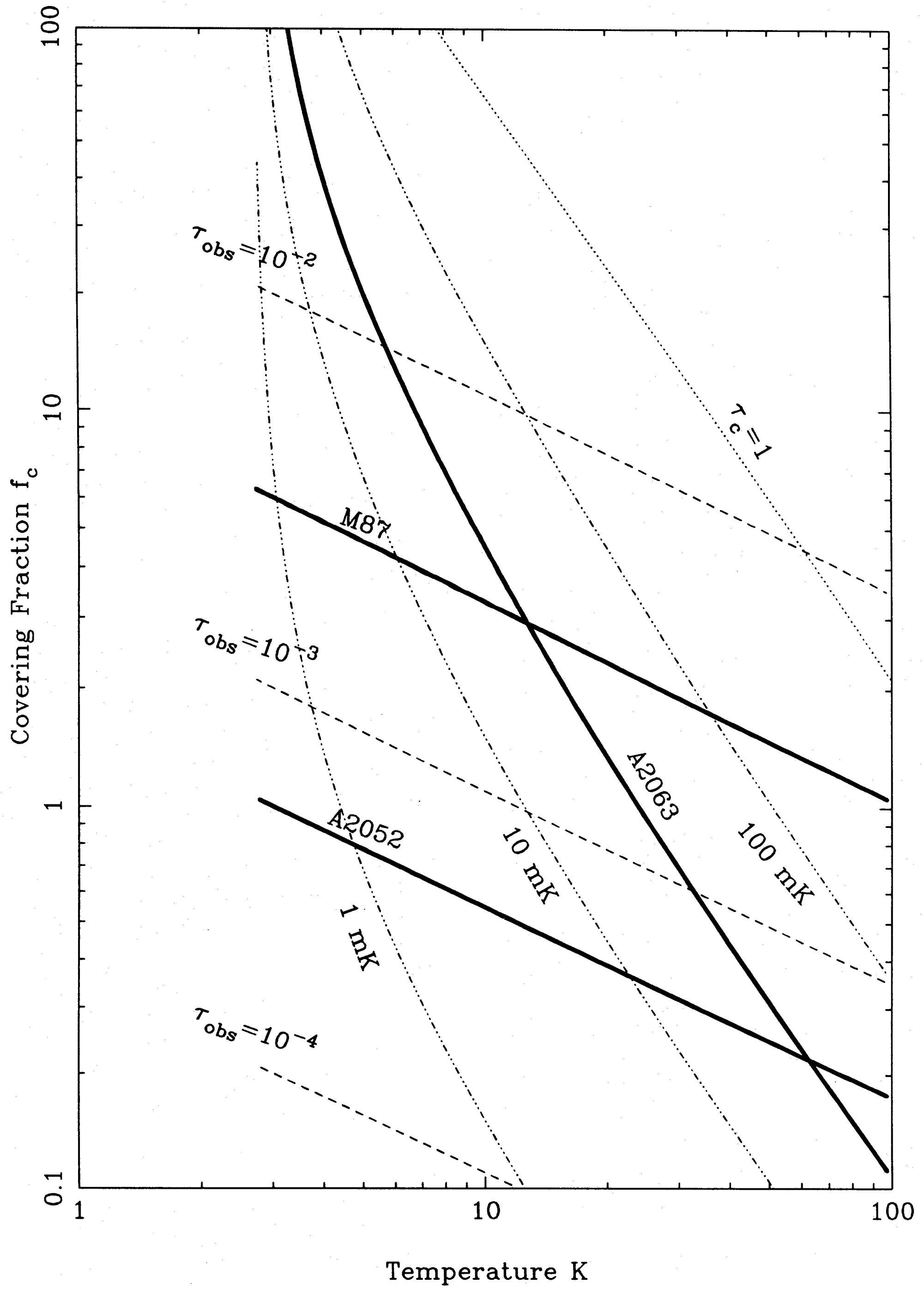

Figure 3. 21-cm signature as a function of covering fraction and assumed H I temperature for a population of pressure-confined, thermal-width clouds with an assumed overall linewidth of 900 km s^{-1}. Dashed lines show the observed optical depth of the cloud population. Dashed-triple dot lines show the antenna temperature of the emission. The solid lines show the emission upper limit measured in A2063 by Valentijn & Giovanelli (1981), and the absorption upper limits for A2052 (Jaffe 1992) and M87 (Allen 1969).

The observed mass of cold, atomic gas within the inner 15 kpc of NGC 1275 must be comparable to or exceed the mass of hot gas. Jaffe (1990) used the Westerbork Synthesis Radio Telescope to map 21-cm absorption across the diffuse, extended radio source in Perseus, using a beam corresponding to about 7×10 kpc^2 (we use $H_0=50$ km s^{-1} Mpc^{-1}, giving an assumed distance of 110 Mpc rather than 71 Mpc as used by Jaffe). He found an absorption feature of large velocity width $\Delta V\approx 500$ km s^{-1} centred on the stellar velocity, and of size approximately 30×10 kpc^2, roughly centred on the nuclear point source, oriented perpendicular to the radio axis and approximately spatially coincident with the regions of emission-line nebulosity with high surface brightness (Lynds 1970; Unger et al. 1990). Jaffe infers an optically thin column density $N_{\mathrm{H\,I}}=1.5\times 10^{21}\,T_{\mathrm{c1}}$ cm^{-2} from his off-nucleus absorption measurements, corresponding to a mass of $\approx 8\times 10^{8}\,T_{\mathrm{c1}}\,\max[1,\,\tau_{\mathrm{c}}]\mathrm{M}_{\odot}$ per 7×10 kpc^2 beam. Even if the H I is optically thin and very cold, $T\sim 10$ K, the mass of cold gas is comparable to the mass of hot gas within the same region, and may exceed it if the cold gas is optically thick, hotter (the upper limit is the brightness temperature of the radio source, ~125 K at Jaffe's position B, the faintest position where absorption is detected), or partly molecular.

The large equivalent width of the observed absorption features requires a large number of clouds along each line of sight $f_c \gtrsim 1000\, T_{c1}^{-1/2}$ in thermal-width clouds, where the equality holds if clouds are optically thick. The observed absorption profiles do not show any significant structure expected if, for instance, the cold clouds were rotationally supported in a disc, and, if the cloud motions are disordered or turbulent, the high covering fraction implies that the mean free path is short and collisions are common.

To complicate the cloud dynamics further, we may interpret the smaller absorption optical depth measured by Jaffe in front of the nucleus of NGC 1275 as a result of the cloud distribution being clumpy, with many clear lines of sight leaving the compact nucleus uncovered. Most of the continuum flux in the beam containing the nucleus is due to the compact nucleus itself, with only about 500 mJy of the total of ≈ 20 Jy provided by the diffuse emission filling the beam (Jaffe 1990, fig. 2a; Pedlar et al. 1990). A clumpy cloud distribution, extending across the diffuse emission within the nuclear beam but leaving the nucleus uncovered, would give an apparent optical depth (diluted by the ratio of fluxes) of 0.0037, within a factor of 2 of that observed. A clumpy cloud distribution with gaps on small scales (smaller than the 1-arcsec resolution of the optical maps but larger than the radio nucleus) also reconciles the surface brightness of the Hα nebulosity, which extends over Jaffe's beam of the nuclear region (Lynds 1970; Caulet et al. 1992) with the lower measured 21-cm optical depth there. Clouds must be clumped on a characteristic scale exceeding the size of the nucleus to give a reasonable probability of leaving the nucleus uncovered. VLBI observations at 18 cm (Kellermann et al. 1971) show that most of the nuclear flux comes from a region smaller than 0.02 arcsec corresponding to 10 pc (the Compton catastrophe limit on the brightness temperature in fact requires that the nucleus has a size of at least 0.003 arcsec), and the mass of such a clump with the required column density $N_{\mathrm{H\,I}} = 1.5 \times 10^{21}\, T_{c1}$ cm^{-2} is $\gtrsim 10^3 (r_c/5\ \mathrm{pc})^2\, T_{c1}\ \mathrm{M}_\odot$. Clumps must have an overall velocity width greater than the absorption equivalent width of 80 km s^{-1}, and hence greater than the sound speed in the cold gas. The clumps are unlikely to be gravitationally bound and are probably magnetically confined, in which case the internal velocity width is determined by the Alfvén velocity, or transient structures due to the mechanism proposed in Section 4.

6 CONCLUSIONS

Excess absorption in the X-ray spectra of cooling flows demonstrates the presence of large masses of heavy elements, principally oxygen, with $M_{\mathrm{metals}} \gtrsim 10^9\ \mathrm{M}_\odot$, distributed out to radii ~100 kpc from the centre of the cooling flow. If still associated with the hydrogen and helium, the mass of cold gas required is large, $\sim 10^{11}\ \mathrm{M}_\odot$. Further evidence for large masses of cold gas in cooling flows, supporting the interpretation of the X-ray absorption as due to cold gas, comes from a 21-cm absorption detection, requiring $\gtrsim 10^{10}\ \mathrm{M}_\odot$ of atomic gas within the inner 15 kpc of the Perseus cluster. We argue that the most consistent physical picture for the X-ray-absorbing material is in the form of an emulsion of small, pressure-confined, magnetized clouds. The survival of clouds relies on magnetic fields, and the dynamics of such clouds are very different from those of clouds in our interstellar medium, as clouds must be suspended and supported in the cluster potential by the hot X-ray-emitting gas, not by centrifugal force.

Mass deposited from the cooling flow is more centrally concentrated than the supporting hot gas where, if star formation is inefficient, dynamically significant masses of cold gas accumulate near the centre of the flow. Large masses of cold gas are likely to be present near the centres of flows, even where the column density of cold material at large radii is too small to cause observable X-ray absorption. A consistent understanding of cloud dynamics must then involve both the hot and cold phase. A high mass fraction of cold clouds will dissipate bulk kinetic energy due to turbulence or sound waves via cloud–cloud collisions. Coagulation and subsequent star formation will be more efficient in the inner regions of the flow, as dissipative cloud collisions in a turbulent medium lead to clumping of clouds. A burst of stirring during a subcluster merger, or powering of a central radio source, may then cause increased star formation and empty the inner regions of accumulated cold gas. Sufficient kinetic energy (via cloud collisions) or thermal energy (as cooling of the hot gas is enhanced by mixing in accumulated cold clouds) can be released to power transiently the emission-line luminosity observed near the centre of some clusters.

If large masses of cold gas extending out to radii of ~100 kpc are a general property of cooling-flow clusters, it can then be puzzling that little cold gas has been detected in H I 21-cm and CO millimetre lines. The few detections in each waveband are consistent with gas present only in the inner ~ 10 kpc of the cooling flow, of similar spatial extent to the emission-line region, not the X-ray-absorbing screen. The other observations give tight upper limits on the mass of cold gas with observational signature similar to cold gas in our Galaxy, far below that required to produce the observed X-ray absorption. The properties of clouds in a cooling flow will be very different, however, and the observational signature per unit mass much lower. Clouds will be colder, and linewidths may be larger. Interpreting the most restrictive H I 21-cm upper limits as limits on the most general population of clouds consistent with the X-ray observations, we still find very little parameter space available for primarily atomic clouds. Calculations of the thermal and chemical equilibrium of dust-free clouds on a population of clouds capable of causing the observed X-ray absorption demonstrate that such clouds will indeed remain mainly atomic, although very cold, with temperatures ~10 K, and a population of such clouds is ruled out, at least in the cluster A2052 with the strongest 21-cm limit. Observational CO limits are similarly restrictive. As significant CO forms only in dusty clouds which are then much colder (with temperatures close to the microwave background temperature), these nevertheless still allow considerable parameter space for plausible cloud populations.

ACKNOWLEDGMENTS

The calculations of cloud thermal structure were performed with the photoionization and gas-phase chemistry code

CLOUDY written by Gary Ferland, and we thank Roderick Johnstone for help and advice with this code. We are grateful to the anonymous referee for drawing our attention to, and G. Miley for communicating, VLA maps of 3C 318.1 in advance of publication. ACF thanks the Royal Society for support. SJD acknowledges support from a pre-doctoral Fellowship funded by the Smithsonian Institution during the completion of this paper, and is grateful to the Center for Astrophysics for providing computer support.

REFERENCES

Allen R. J., 1969a, A&A, 3, 316
Allen R. J., 1969b, A&A, 3, 382
Allen S. W., Fabian A. C., Johnstone R. M., Nulsen P. E. J., Edge A. C., 1992, MNRAS, 254, 51
Allen S. W., Fabian A. C., Johnstone R. M., White D. A., Daines S. J., Edge A. C., Stewart G. C., 1993, MNRAS, 262, 901
Binggeli B., Tammann G. A., Sandage A., 1987, AJ, 94, 251
Bregman J. N., Hogg D. E., 1988, AJ, 96, 455
Bregman J. N., Roberts M., 1990, ApJ, 362, 468
Bregman J. N., McNamara B. R., O'Connell R. W., 1990, ApJ, 351, 406
Burns J. O., White R. A., Haynes M. P., 1981, AJ, 86, 1
Caulet A., Woodgate B. E., Brown L. W., Gull T. R., Hintzen P., Lowenthal J. D., Oliversen R. J., Ziegler M. M., 1992, ApJ, 388, 301, 29
Crane P. C., van der Hulst J. M., Haschick A. D., 1982, in Heeschen D. S., Wade C. M., eds, Proc. IAU Symp. 97, Extragalactic Radio Sources. Reidel, Dordrecht, p. 307
Crawford C. S., Fabian A. C., 1992, MNRAS, 259, 265
Edge A. C., Stewart G. C., Fabian A. C., 1992, MNRAS, 258, 177
Fabian A. C., Hu E. M., Cowie L. L., Grindlay J., 1981, ApJ, 248, 47
Fabian A. C., Nulsen P. E. J., Canizares C. R., 1984, Nat, 311, 733
Fabian A. C., Nulsen P. E. J., Canizares C. R., 1991, A&AR, 2, 191
Fabian A. C., Daines S. J., Johnstone R. M., 1994, MNRAS, submitted
Ferland G., 1993, University of Kentucky Department of Physics and Astronomy Internal Report
Ferland G., Fabian A. C., Johnstone R. M., 1994, MNRAS, 266, 399
Field G. B., 1958, Proc. I.R.E., 46, 240
Ge J. P., Owen F. N., 1993, AJ, 105, 778
Gilden D. L., 1984, ApJ, 279, 335
Grabelsky D. A., Ulmer M. P., 1990, ApJ, 355, 401, 3
Haynes M. P., Brown R. L., Roberts M. S., 1978, ApJ, 221, 414
Heckman T. M., Baum S. A., van Breugel W. J. M., McCarthy P., 1989, ApJ, 338, 48
Holtzmann J. A. et al., 1992, AJ, 103, 691
Hu E. M., Cowie L. L., Wang Z., 1985, ApJS, 59, 447
Jaffe W., 1987, A&A, 171, 378
Jaffe W., 1990, A&A, 240, 254
Jaffe W., 1991, A&A, 250, 67
Jaffe W., 1992, in Fabian A. C., ed., Clusters and Superclusters of Galaxies. Kluwer, Dordrecht, p. 109
Jaffe W., 1994, A&A, in press
Jaffe W., de Bruyn A. G., Sijbreng D., 1988, in Fabian A. C., ed., Cooling Flows in Clusters and Galaxies. Kluwer, Dordrecht, p. 63
Johnstone R. M., Fabian A. C., 1988, MNRAS, 233, 581
Johnstone R. M., Fabian A. C., Edge A. C., Thomas P. A., 1992, MNRAS, 255, 431
Kaplan S. A., Pikelner S. B., 1970, The Interstellar Medium. Harvard Univ. Press, Cambridge, Massachusetts, p. 53
Kellermann K. I. et al., 1971, ApJ, 169, 1
Kim K. T., Tribble P. C., Kronberg P. P., 1991, ApJ, 379, 80
Lazareff B., Castets A., Kim D.-W., Jura M., 1989, ApJ, 336, L13
Loewenstein M., Fabian A. C., 1990, MNRAS, 242, 120
Lynds R., 1970, ApJ, 159, L151
McNamara B. R., Jaffe W., 1994, A&A, 281, 673
McNamara B. R., Bregman J. N., O'Connell R. W., 1990, ApJ, 360, 20
Mathews W. G., Murray S. D., 1987, ApJ, 312, 66
Mirabel I. F., Sanders D. B., 1989, ApJ, 340, L9
Mushotzky R. F., 1992, in Fabian A. C., ed., Clusters and Superclusters of Galaxies. Kluwer, Dordrecht, p. 91
Nulsen P. E. J., 1986, MNRAS, 221, 377
O'Dea C. P., Baum S. A., Maloney P. R., Tacconi L. J., Sparks W. B., 1994, ApJ, 422, 467
Pedlar A., Ghataure H. S., Davies R. D., Harrison B. A., Perley R., Crane P. C., Unger S. W., 1990, MNRAS, 246, 477
Penzias A. A., Scott E. H., 1968, ApJ, 153, L7
Pringle J. E., 1989, MNRAS, 239, 479
Quintana H., Melnick J., Infante L., Thomas B., 1985, AJ, 90, 410
Raymond J. C., Smith B. W., 1977, ApJS, 35, 419
Richer H. B., Crabtree D. R., Fabian A. C., Lin D. N. C., 1993, AJ, 105, 877
Sarazin C. L., 1988, X-ray Emission from Clusters of Galaxies. Cambridge Univ. Press, Cambridge
Thomas P. A., Fabian A. C., Nulsen P. E. J., 1987, MNRAS, 228, 973
Unger S. W., Taylor K., Pedlar A., Ghataure H. S., Penston M. V., Robinson A., 1990, MNRAS, 242, 33P
Valentijn E. A., Giovanelli R., 1982, A&A, 114, 208
White D. A., Fabian A. C., Johnstone R. M., Mushotzky R. F., Arnaud K. A., 1991, MNRAS, 252, 72
Zabludoff A. I., Huchra J. P., Geller M. J., 1990, ApJS, 74, 1

APPENDIX A: A SIMPLE COOLING-FLOW PARAMETRIZATION

Observations of the surface brightness profile of cooling flows show that it is less centrally peaked than expected if all the cooling gas flows into the centre. The gas is required to be inhomogeneous and multiphase, with gas initially on a range of adiabats so that blobs of gas cool below X-ray temperatures and drop out from the flow at a range of radii as the gas flows inwards. We give here a simple parametrization of the observed properties of a cooling flow, as derived from deprojection of the X-ray surface brightness profile (Fabian et al. 1981; Thomas, Fabian & Nulsen 1987). We take the density (of nuclei) at radius $100R_2$ kpc to be

$$n_{\rm h}(R)=\begin{cases}4.0\times10^{-3}R_2^{-2}n_{-2.40}\ {\rm cm}^{-3}, & 0.1<R_2<2,\\ 4.0\times10^{-3}[1+(R_2/2)^2]^{-1}n_{-2.40}\ {\rm cm}^{-3}, & R_2>2,\end{cases}\tag{A1}$$

where $10^{-2.40}n_{-2.40}$ cm^{-3} is the density of nuclei at 100 kpc (for completeness we have joined on a King law with core radius 200 kpc outside the cooling flow at $R_2>2$). The mass of hot gas within radius R is given by

$$M_{\rm h}(r)=8.2\times10^{11}R_2^2 n_{-2.40}\ {\rm M}_\odot,\qquad 0.1<R_2<2.\tag{A2}$$

The temperature and hence pressure within the cooling flow are the least well-determined from deprojection of imaging data, as they depend on the depth of the assumed potential. We assume that the temperature of the hottest gas phase $T_{\rm h}=10^{7.7}T_{\rm h7.7}$ K is roughly constant, giving a pressure of

$$P_{\rm h}(R)\approx4.1\times10^5R_2^{-1}n_{-2.40}T_{\rm h7.7}\ {\rm cm}^{-3}\,{\rm K},\qquad 0.1<R_2<2.\tag{A3}$$

The cooling time at radius R is

$$t_{\rm cool}(R) \approx 1.0 \times 10^{10} R_2 n_{-2.40}^{-1} T_{\rm h\,7.7} \Lambda_{-23.4}^{-1}\ {\rm yr}, \qquad 0.1 < R_2 < 2, \tag{A4}$$

where we have taken the cooling function $\Lambda = 10^{-23.4} \Lambda_{-23.4}$ erg cm^3 s^{-1} for a 0.4 solar metallicity gas at temperature $10^{7.7}$ K (Raymond & Smith 1977). The cooling radius, where $t_{\rm cool} = 2 \times 10^{10}$ yr, is then $R_{\rm cool} = 196\, n_{-2.40} T_{\rm h\,7.7}^{-1} \Lambda_{-23.4}$ kpc. Within the cooling radius the cooling flow is approximately in a steady state, and the inferred mass deposition rate (ignoring gravitational work) within radius R is given approximately by dividing the X-ray luminosity within this radius, $L_{\rm x}(R) = 1.0 \times 10^{44} R_2 n_{-2.40}^2 \Lambda_{-23.4}$ erg s^{-1}, by the enthalpy of the inflowing gas, giving

$$\dot{M}(R) \approx 100 R_2 n_{-2.40}^2 \Lambda_{-23.4} T_{7.7}^{-1}\ {\rm M}_\odot\ {\rm yr}^{-1}, \qquad 0.1 < R_2 < 2. \tag{A5}$$

Mass deposition probably continues somewhat beyond the cooling radius, as some of the multiphase gas can be cooling even when the emission-weighted cooling time exceeds a Hubble time (Thomas et al. 1987). The mean inflow velocity $v_{\rm flow}(R) = 6.0\, n_{-2.40} \Lambda_{-23.4} T_{\rm h\,7.7}^{-1}$ km s^{-1} is highly subsonic everywhere and, in a multiphase flow where mass drops out with decreasing R, does not increase dramatically towards the centre (in this particular parametrization it is independent of radius).

If star formation is negligible and the cooled gas remains at the radius where it was deposited from the flow, then the averaged density of deposited cold gas at radius R after time $10^{10} t_{10}$ yr is $\bar{n}_{\rm c}(R, t) \approx 2.3 \times 10^{-3} R_2^{-2} t_{10} n_{-2.40}^2 \Lambda_{-23.4} T_{\rm h\,7.7}^{-1}$ cm^{-3}. Alternatively, we might perhaps expect cold clouds to be advected inwards with the mean flow (which could also concentrate pre-existing cold clouds), and the mean density then satisfies the advection equation

$$R^2 \frac{\partial \bar{n}_{\rm c}(R, t)}{\partial t} = R^2 \dot{n}_{\rm c}(R) + \frac{\partial [R^2 v_{\rm flow} \bar{n}_{\rm c}(R, t)]}{\partial R}, \tag{A6}$$

where $\dot{n}_{\rm c}(R, t) \propto R^{-2}$ is the rate of mass injection from the flow. If $v_{\rm flow}$ is constant, then the flow will focus cold clouds so that $\bar{n}_{\rm c} \propto R^{-2}$. The solution for averaged cold gas density accumulated at radius R in an initially empty cooling flow after time t is $\bar{n}_{\rm c}(R, t) \propto R^{-2} t$, and is identical for the two cases where cold clouds remain where they are deposited or are advected inwards.

The parametrization above may be scaled for a less-massive cooling flow by substituting $n_{\rm h} \rightarrow n_{\rm h}/2$ and $T_{\rm h} \rightarrow T_{\rm h}/2$, giving $\dot{M}(R) \rightarrow 0.38 \dot{M}(R)$ and $R_{\rm cool} \rightarrow 0.76 R_{\rm cool}$.